Modeling the Circle of Willis Using Electrical Analogy Method under both Normal and Pathological Circumstances

Abdi M.[1], Karimi A.[1], Navidbakhsh M.[1], Rahmati M. A.[2], Hassani K.[3], Razmkon A.[4*]

[1]Department of Mechanical Engineering, Iran University of Science and Technology, Tehran 16844, Iran
[2]Department of Biomedical Engineering, Amirkabir University of Technology, Tehran 14987, Iran
[3]Department of Biomechanics, Science and Research Branch, Islamic Azad University, Tehran 12569, Iran
[4]Shiraz Neuroscience Research Center, Department of Neurosurgery, Shiraz University of Medical Sciences, Shiraz, Iran

ABSTRACT

Background and objective: The circle of Willis (COW) supports adequate blood supply to the brain. The cardiovascular system, in the current study, is modeled using an equivalent electronic system focusing on the COW.

Method: In our previous study we used 42 compartments to model whole cardiovascular system. In the current study, nevertheless, we extended our model by using 63 compartments to model whole CS. Each cardiovascular artery is modeled using electrical elements, including resistor, capacitor, and inductor. The MATLAB Simulink software is used to obtain the left and right ventricles pressure as well as pressure distribution at efferent arteries of the circle of Willis. Firstly, the normal operation of the system is shown and then the stenosis of cerebral arteries is induced in the circuit and, consequently, the effects are studied.

Results: In the normal condition, the difference between pressure distribution of right and left efferent arteries (left and right ACA–A2, left and right MCA, left and right PCA–P2) is calculated to indicate the effect of anatomical difference between left and right sides of supplying arteries of the COW. In stenosis cases, the effect of internal carotid artery occlusion on efferent arteries pressure is investigated. The modeling results are verified by comparing to the clinical observation reported in the literature.

Conclusion: We believe the presented model is a useful tool for representing the normal operation of the cardiovascular system and study of the pathologies.

Keywords

Artery occlusion, Cardiovascular system, Cerebrovascular system, Collateral vessel, Pressure waveforms

Introduction

The human cardiovascular system diseases are considered as one of the main problems and challenges in contemporary health care in industrial countries. They bring about the majority of deaths and also often suffer people in their most productive age. Blood vessels supplying the human brain consist of two isolated vascular systems: vertebral–basilar arteries (VBAs) and internal carotid arteries (ICAs). In the base of the brain both systems of arteries are connected bilaterally by posterior communicating arteries (PCOAs) and left–to–right side by anterior communicating artery (ACOA) forming the so called circle of Willis (COW). The anatomical specificity of cerebral arterial supply consists of several nodes in which arteries join or bifurcate and spatial tortuosity (siphon–shaped sections) of ICA and vertebral arteries. In

*Corresponding author:
Razmkon A.
Shiraz Neuroscience Research Center, Department of Neurosurgery, Shiraz University of Medical Sciences, Shiraz, Iran
P.O.Box 71455-166, Shiraz, IRAN.
E-mail: ali.razmkon@gmail.com

terms of hydrodynamics, this is an extremely complicated flow. The main branches of the COW are segments of the anterior cerebral arteries (ACAs–A2), the middle cerebral arteries (MCAs), and the posterior cerebral arteries (PCAs–P2). In patients with severe carotid or vertebral artery disease, several collateral pathways may contribute to cerebral perfusion [1]. However, collateral flow via the C–W seems to be of primary importance [2]. Insufficient cerebral blood flow due to local occlusion of supplying arteries or anterior communicating artery aneurysm [3] may lead to irreversible brain damage [4]. Physical and Mathematical models of cerebral circulation can be used for simulation purpose [5, 6]. Different approach such as experimental approach, 1–D, 2–D, or three dimensional simulations and electrical analogy method approach were used to study cardiovascular system and effects of diseases on it [7-9]. In this study, electrical analogy method is utilized with the aim of providing better perception and simulation of the blood pressure distribution in the human cardiovascular system which will lead to reliable outcomes. The preliminary computer models explaining the arterial system were constructed a multi branched model of the systemic arterial tree allowed modeling of different physiological and pathological conditions. This model was extended in detail later [10]. By utilizing computer aided design, then control systems were developed to produce applicable electrical analogy of the human cardiovascular system. Furthermore, a model of cerebrovascular reactivity including the Circle of Willis and Cortical anastomoses is developed [11]. It has been used to simulate steady–state circulatory circumstance with transients introduced by varying the peripheral resistance [12]. A transient computer model for flow and pressure ranges in the human cardiovascular system was assessed [13]. The simulation of steady state and transient condition using the electrical analogy has also been managed but the arteries have not been included in their model widely [14]. The 1–D axisymmetric Navier–Stokes equations for transient blood flow in a rigid vessel had been used to derive lumped models relating flow and pressure propagation [15]. In our previous study, we have modeled the normal operation of cardiovascular system using a 42 compartment model [16], nevertheless, the problem was that the model elements were passive because of using voltage sources.

In this study, we tried to advance the previous model by adding new cerebral compartments and introduced a 63 compartments model representing the whole cardiovascular system. The blood pressure distribution of efferent arteries (ACAs–A2, MCAs, and PCAs–P2) is investigated under both normal and stenosis condition. Our study consists of the following steps:

a) The presentation of block diagram of cardiovascular system.

b) The design of the electronic cardiovascular system based on the block diagram.

c) The pressure distribution of six efferent arteries, including right and left anterior cerebral arteries (ACAs–A2), right and left middle cerebral arteries (MCAs), and finally right and left posterior cerebral arteries (PCAs–P2) are obtained to analyze the impact of anatomical difference at left and right section of supplying arteries of COW on pressure distribution of left and right efferent arteries. In addition, the effect of internal carotid artery occlusion on efferent arteries pressure is investigated.

d) The verification of the results with the relevant experimental and clinical observations is conducted.

Materials and Methods

The block diagram of cardiovascular system is displayed in Figure 1. This is a real presentation of physiological cardiovascular system. Cardiovascular system includes the left and right ventricles, left and right atriums, pulmonary system, arteries, and set of capillaries, veins and cerebrovascular system.

In this present study, we focused on cerebro-

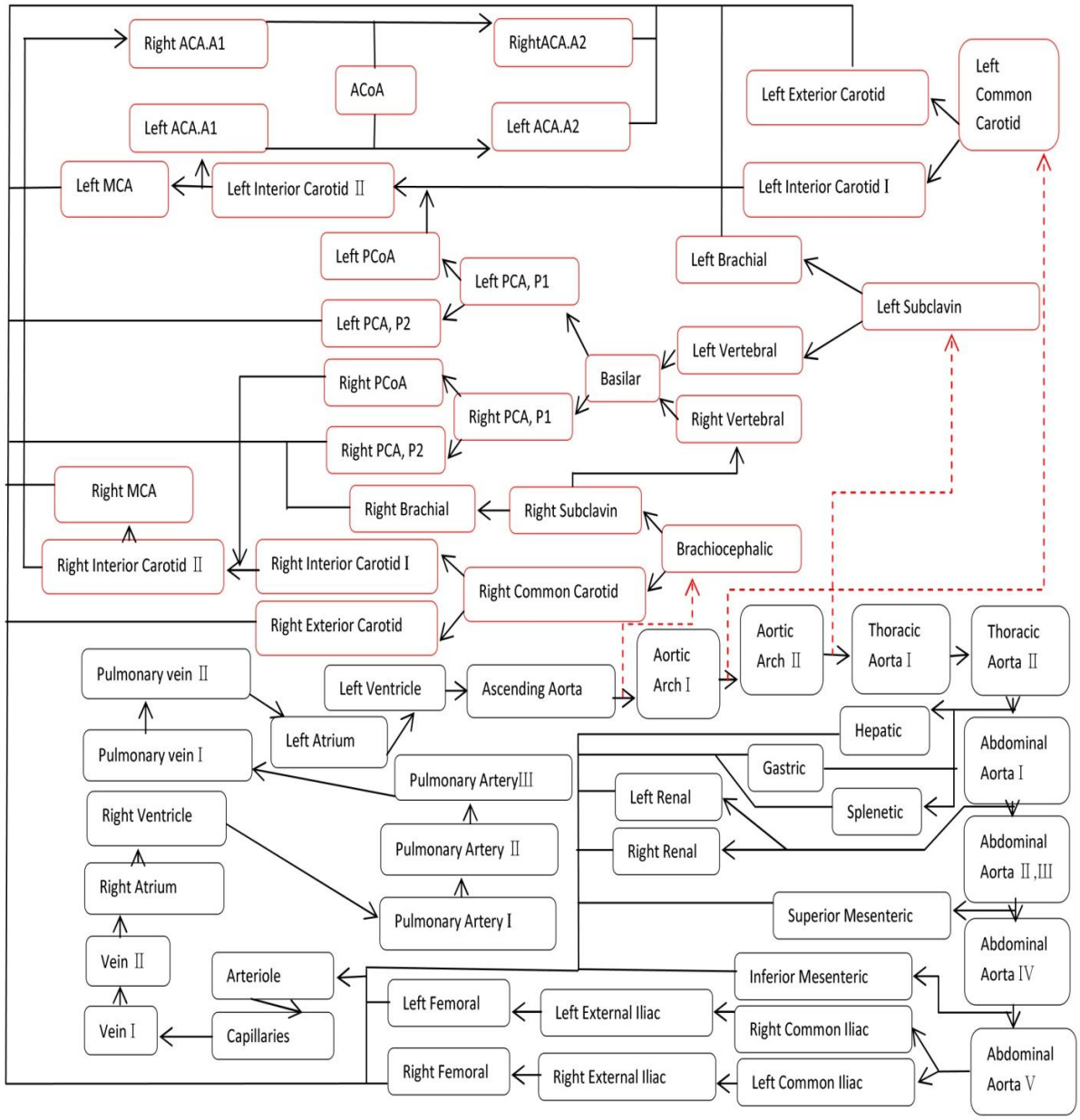

Figure 1: Block diagram of the cardiovascular system including previous system mentioned in reference [19] and circle of Willis.

vascular system which begins at the largest arteries supply the circle of Willis follows by circle of Willis arteries and finally ends with efferent arteries as a subset of cardiovascular system. The rest of cardiovascular system is only considered to apply inflow and outflow pressure to cerebrovascular system.

Each vessel, atrium and set of all capillaries, and arterioles has been presented by an element, including resistor, inducer, and capacitor.

The model is composed of 63 compartments. The equivalent circuit of the COW system is demonstrated in Figure 2 (A), but whole cardiovascular system except COW system is shown in Figure 2 (B) in which connection with the COW system is presented by red dashed lines.

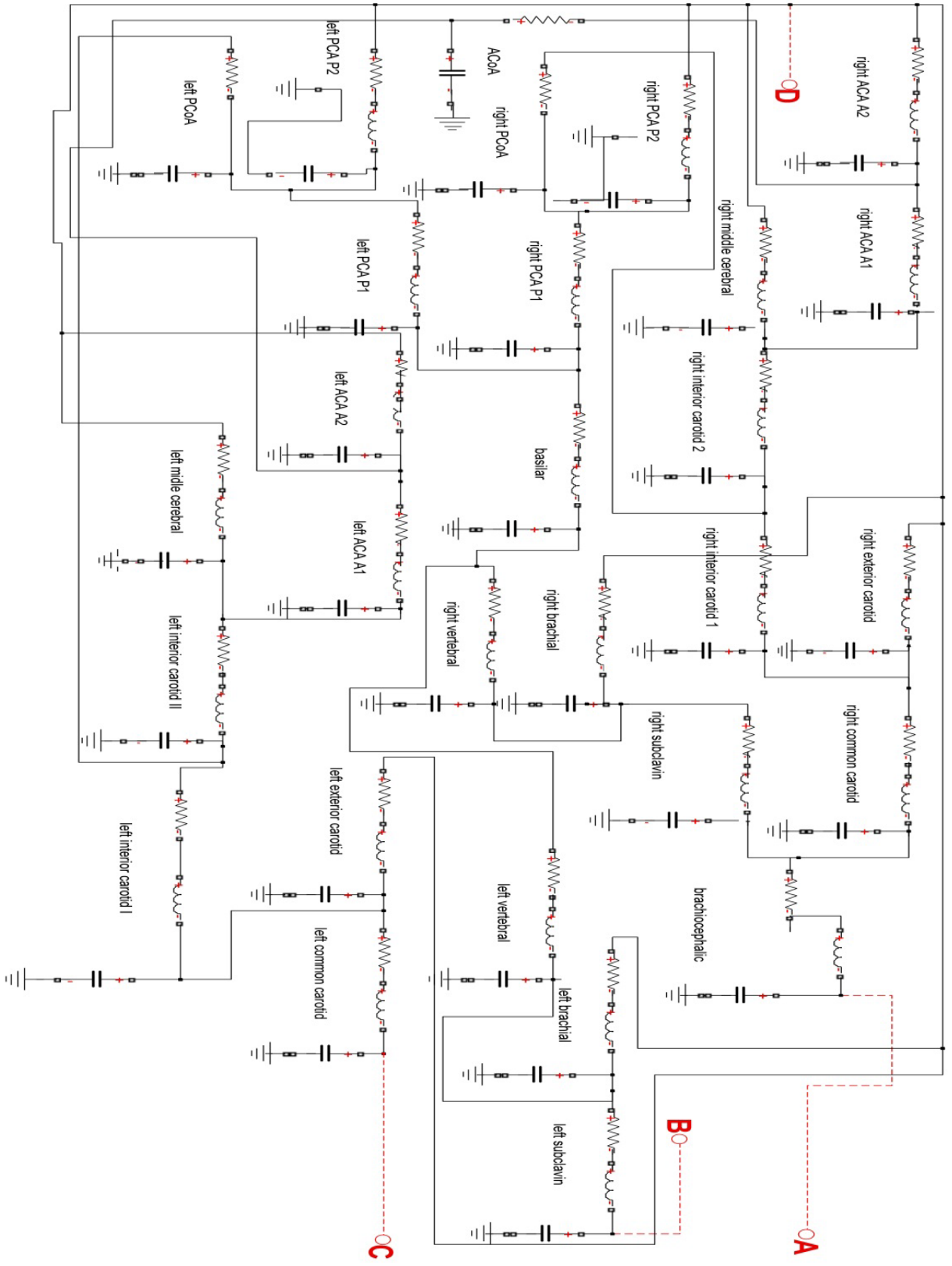

Figure 2 (A): Electronic circuit of cerebral vascular system that is connected to the main cardio-vascular, depicted by red dashed lines.

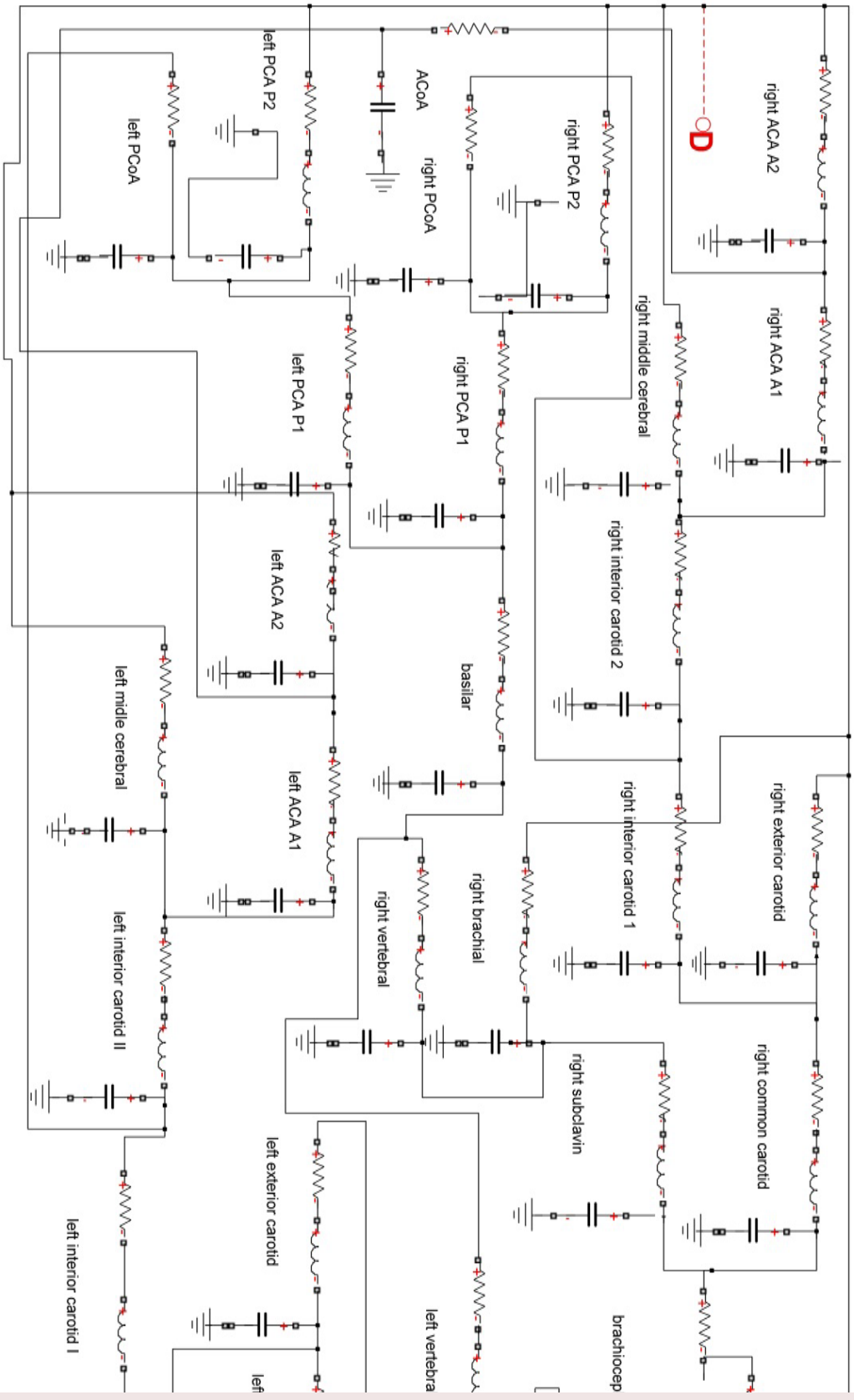

Figure 2 (B): Electronic circuit of whole cardiovascular system except cerebrovascular system.

Brachiocephalic artery originates from ascending aorta artery followed by right common carotid. Left common carotid originates from aortic arch 1 and, left subclavin derived from aortic arch 2. This development and using proper artery originations are performed in this paper according to references [17, 18] that was not considered in literature [18]. We illustrated the whole cardiovascular system compartments in Figure 1 to show improvements more exactly.

The primary parameters such as length, elastic modulus, area, thickness, density, blood viscosity for ventricles, pulmonary artery, veins, arterioles, capillaries, and atriums (whole cardiovascular system except cerebrovascular system) have been obtained [14] and electrical characteristics of the cardiovascular system, except COW, were extracted and used [16].

The values of resistance (R), capacitance (C) as well as inductance (L) for COW are calculated using following relations [18]:

$$R=8l\mu/A^2 \quad (1)$$

where l and A are the length and cross section area and μ is the blood viscosity;

$$C=3l\pi r^3/2Eh \quad (2)$$

where E and h are the elastic modulus and thickness of artery, respectively.

$$L=9l\rho/4A \quad (3)$$

where ρ is the blood density;

The initial values such as length, radius, thickness, and elastic modulus for cerebrovascular system were derived from J. Alastruey et al. study [17].

Using the electrical circuit, we simulated the normal operation of cardiovascular system by MATLAB and the effects of the cerebral stenosis is also modeled by changing left internal carotid radius and recalculating of resistance, inductance, and compliance values. The pressure graphs of the cardiovascular system as well as the pressure propagations at efferent arteries are obtained.

The left and right ventricular pulse pressures are considered as input (Figure 3). The input voltage is controlled by the voltage source. In fact, we convert the left and right ventricle pressure waveform to equivalent voltage propagation. Left ventricle pressure varies between 5 and 140 mmHg and follows a sinusoidal pattern. The pressure of right ventricle, moreover, varies between 5 and 30 mmHg. Left and right ventricular pressures are derived and compared to relevant experiments [15, 18] shown in Figures 4 and Figure 5. Since the circuit input is a voltage source, therefore, the output at the efferent arteries is the pressure propagation. Arterial pressure is one the main parameters which has prognostic value [20] and can be used as an indicator in human cardiovascular system modeling.

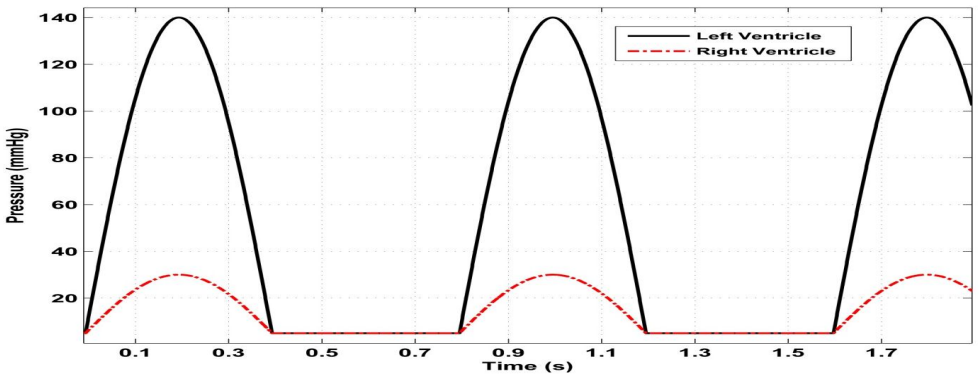

Figure 3: The left and right ventricular pulse pressures are considered as input.

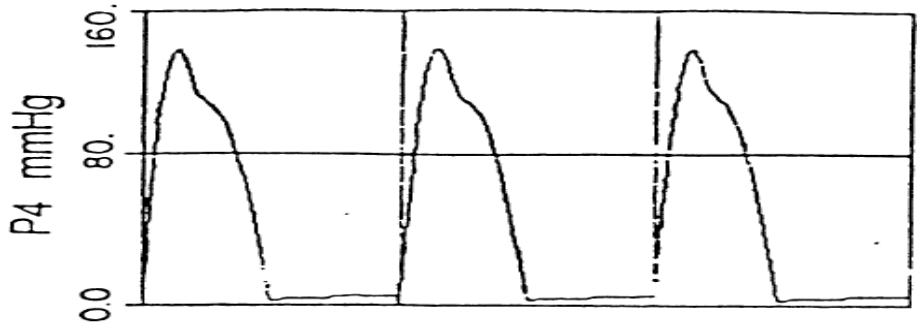

Figure 4: The left ventricular pulse pressure –time graph [17]

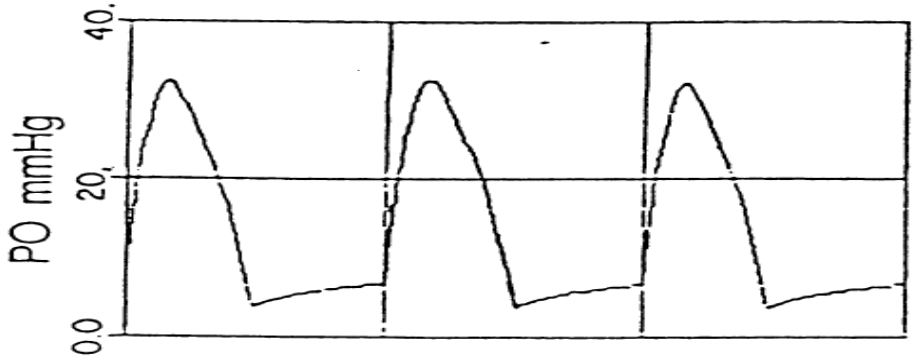

Figure 5: The right ventricular pulse pressure –time graph [17]

Results

Pressure wave propagation in efferent arteries under normal condition

The pressure–time graph of left and right anterior cerebral arteries are shown in Figure 6, where the waveform varies between 67–95.84 mmHg (volt) and 67–94.87mmHg (volt), respectively. The waveform starts from 67 mmHg and the peak is in 94.87 mmHg for right and 95.84 mmHg for left. Our model is also able to predict the in vivo observed pressure patterns at the left and right middle cerebral arteries. The pressure of left and right middle cerebral arteries is shown in Figure 7. This graph shows that middle cerebral artery pressure varies between 99.87 mmHg (dias-

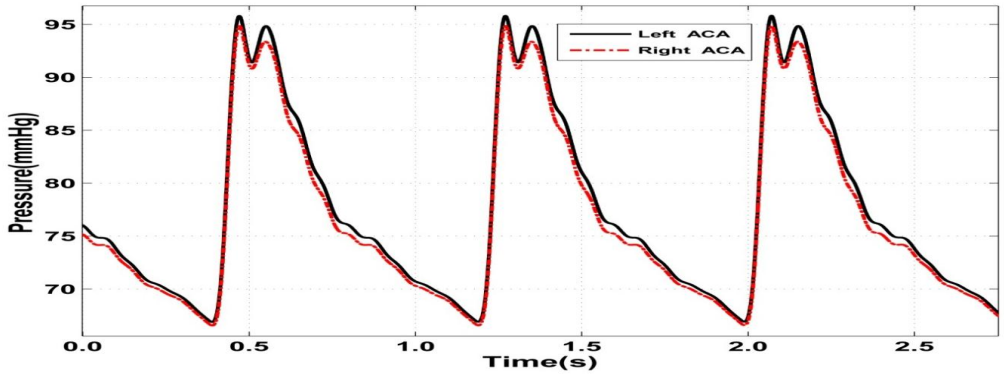

Figure 6: Pressure-time graph of left and right anterior cerebral arteries.

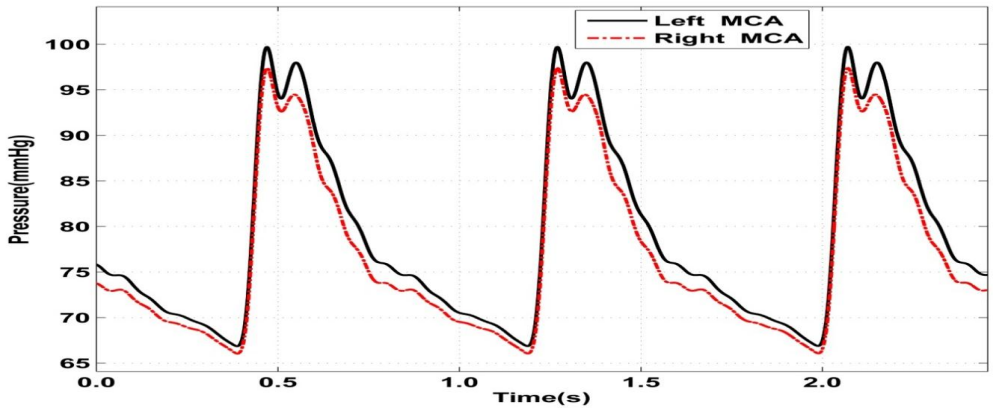

Figure 7: Pressure-time graph of left and right middle cerebral arteries.

tole–systole) and 68–97.46 mmHg for left and right arteries, respectively.

Finally, in this section we investigated the pressure distribution in left and right posterior cerebral arteries. Figure 8 indicates the left and right pressure of posterior cerebral arteries varies between 67–97 mmHg (diastole–systole).

Pressure wave propagation in efferent arteries under pathological condition

The maximum amount of pressure in Figures 9 and Figure 10 are 88.77 mmHg and 85.52

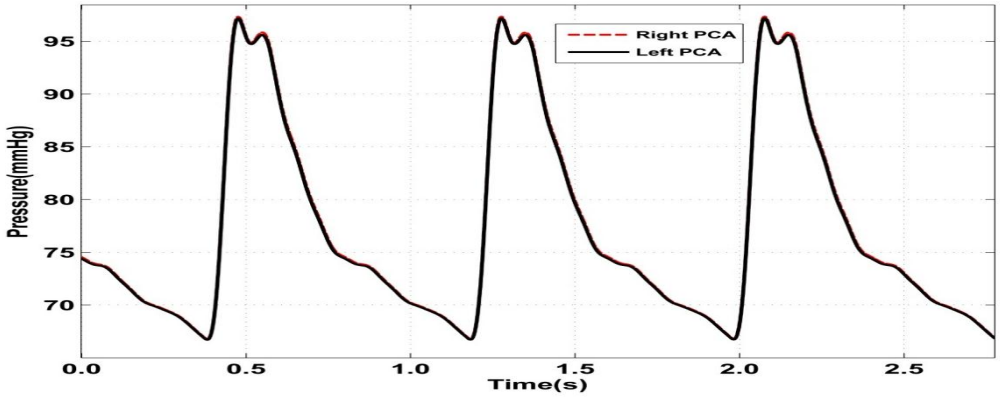

Figure 8: Pressure-time graph of left and right posterior cerebral arteries.

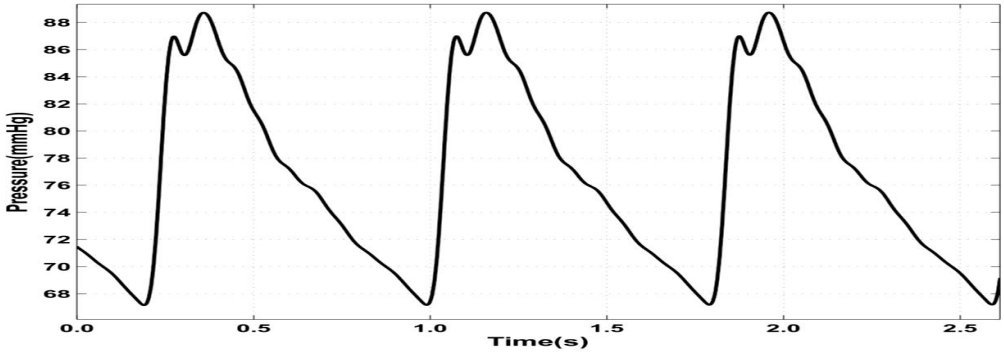

Figure 9: Pressure-time graph of left middle cerebral artery in the case of 50% rate of occlusion introduced in left internal carotid artery.

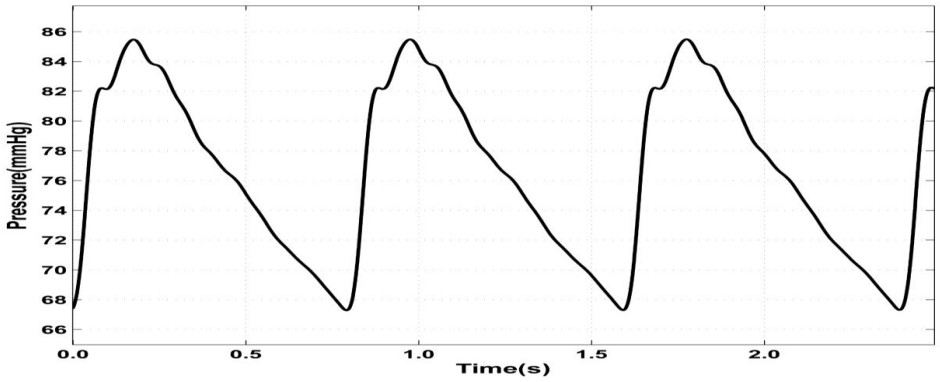

Figure 10: Pressure-time graph of left middle cerebral artery in the case of 100% rate of occlusion (completely occlusion) introduced in left internal carotid artery.

mmHg, respectively.

Figure 11 depicts maximum pressure (during systole) in six efferent arteries as a function of incremental rate of the left internal carotid artery occlusion. All six efferent arteries present descending trends.

Discussion

Under normal condition

The results of the simulation performed based upon left and right ventricle pressure variations mimicking by controlled voltage source (voltage is equivalent blood pressure in electrical analogy method).

To validate our model, we compared the results to the reference [17] as shown in Figure 12 (B). Pressure–time diagram of brachiocephalic artery which indicates [17] is the only guideline that we could use for the comparison. However, three pressure–time diagrams of Brachiocephalic, subclavin, and common carotid arteries are shown, but we only focused on the first one. Diagrams of these arteries, as referenced, should not be similar to each other because they are originated from different parts of aorta artery, and then minor differences naturally should be found. We noticed the pressure at vertical axis of Brachiocephalic artery diagram in the reference changes between 10 and 17 KPa, although calculated pressure in this study in the vertical axis varies between 9.5 and 16.2 KPa. It means that our diagram is shifted slightly downward. This difference

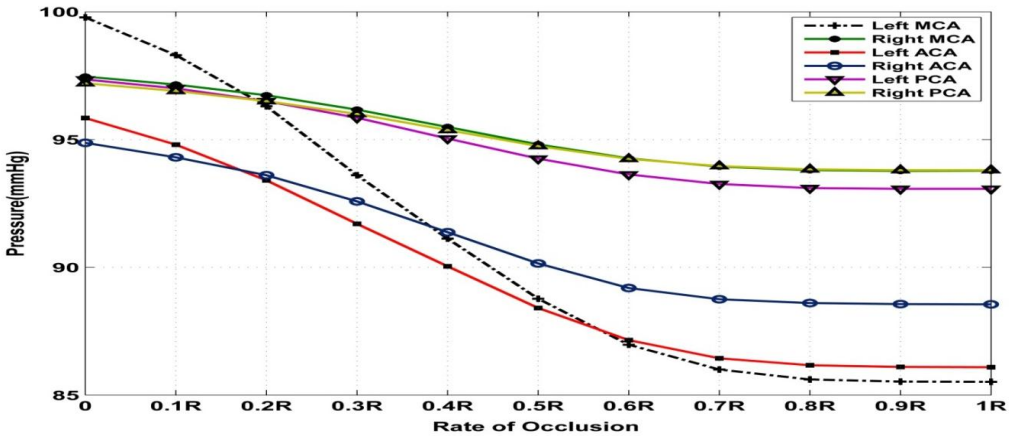

Figure 11: Maximum pressures (during systole) in six efferent arteries as a function of incremental rate of occlusion of the left internal carotid artery.

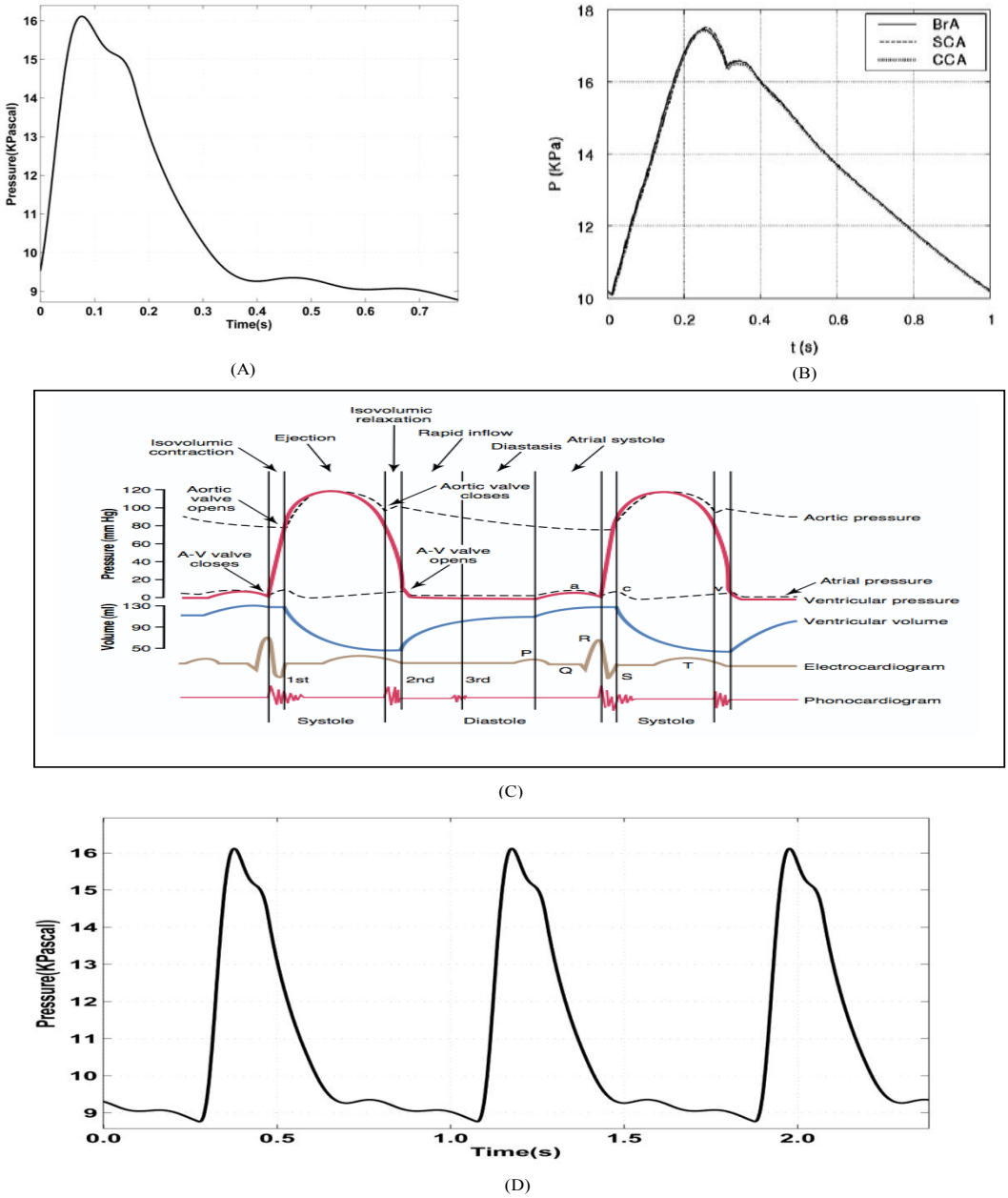

Figure 12: Pressure-time graph of brachiocephalic artery is obtained for one cycle (A) is compared to curve extracted from literature (B) [16]. Part C depicts aorta artery pressure-time variation [14]. Part D shows brachiocephalic artery pressure-time graph for more cycles.

could be related to the solution method which the problem is solved. In both diagrams there are similarities. For example, both are shown two peaks, although in both of them basically there are clearly some differences in pattern. The reference diagram after two peaks with slight slope moves downward the minimum amount. However, this pattern is not correct since: firstly, heart period in the reference diagram is 1 second as default which should be 0.8 second; as we applied in our diagram, the second is that if we look at the aorta artery diagram in another reference [14] in figure 12 (C) we can come up with this conclusion that in

the systole, the first 0.3 second, the diagram is at the maximum value and then after that is at the minimum amount moving with the constant slope. We expect to see this fluctuation pattern in brachiocephalic artery. This pattern is seen in the pressure diagram illustrated by us but is not shown in the reference diagram [16].

Simulation results performed under normal conditions for cardiovascular system are presented in Figure 6 to Figure 8. We analyzed pressure wave propagation along efferent arteries. The results are in agreement with experimental observation [20]. Our model predicts similar pressure patterns in efferent arteries (left and right anterior cerebral arteries, left and right middle cerebral arteries) of the complete COW. In Figures 6 and 7, there is difference between the same efferent arteries at both sides of the COW which indicates that pressure distribution in the cerebral arteries are affected by the asymmetry introduced by the brachiocephalic artery. The values and distribution of these pressures are within acceptable physiological ranges compared to average experimental measurements calculated in literature [20]. Pressure value and distribution in left and right posterior cerebral arteries are approximately the same (Figure 8), because no asymmetry sign is seen in originating artery (basilar artery). As the previous results, these results are in agreement with experimental and numerical articles [20].

Under cerebral stenosis condition

If the rate of internal carotid artery occlusion increases, the maximum amount of pressure decreases (Figures 9 and 10). Also the pressure fluctuation pattern in the normal condition and in the condition with different rate of occlusion is completely distinct. Figure 11 shows maximum pressure (during systole) in six efferent arteries as a function of incremental rate of the left internal carotid artery occlusion. In all cases, the left one has a greater value than the one on the right under normal condition (0R) and the right one has higher amount in complete occlusion (1R). The left middle cerebral artery depicts the highest reduction rate in pressure and is followed by left anterior cerebral artery. Middle cerebral artery receives blood supply more than L.ACA, because of three main reasons:

a) Straight connection between L.MCA and L.ICA.

b) L.MCA is the first outflow artery to be supplied by L.ICA.

c) L.MCA has bigger diameter than L.ACA.

The left and right posterior cerebral arteries have no direct connection with left internal carotid artery and originate from basilar artery; hence, occlusion impact on these arteries is less than others. In all six efferent arteries, changing rate at right pressure value is less than the left one.

Conclusion

We believe the presented model is a useful tool for representing the normal operation of the cardiovascular system and study of the pathologies. We only considered one type of pathology namely stenosis of the cerebral arteries but the circuit is able to show different pathologies. In a nutshell, we hope to extend this model to predict the flow in arteries at different conditions, including exercise and diseases.

Acknowledgement

The authors acknowledge all the help and support of their colleagues at Iran University of Science and Technology, National Institute of Genetic Engineering and Biotechnology, and Amirkabir University of Technology.

Funding: This project was supported by the grant 160/455 from Iran University of Science and Technology and 440 from National Institute of Genetic Engineering and Biotechnology.

Conflict of Interest

We declare that we have no competing inter-

est.

References

1. MacIntosh BJ, Sideso E, Donahue MJ, et al. Intracranial Hemodynamics Is Altered by Carotid Artery Disease and After Endarterectomy: A Dynamic Magnetic Resonance Angiography Study. *Stroke* 2011 Apr; **42**(4): 979-84. doi:10.1161/STROKEAHA.110.590786. Epub 2011 Feb 24.PubMed PMID: 21350206.
2. Hoksbergen AW, Fülesdi B, Legemate DA, Csiba L. Collateral configuration of the circle of Willis: transcranial color-coded duplex ultrasonography and comparison with postmortem anatomy. *Stroke* 2000 Jun; **31**(6): 1346-51. PubMed PMID:10835455.
3. Jou LD, Lee DH, Mawad ME. Cross-flow at the anterior communicating artery and its implication in cerebral aneurysm formation. *J Biomech* 2010 Aug 10; **43**(11): 2189-95. doi: 10.1016/j.jbiomech.2010.03.039. Epub 2010 May 5. PubMed PMID: 20447636.
4. Fahrig R, Nikolov H, Fox AJ, Holdsworth DW. A three-dimensional cerebrovascular flow phantom. *Med Phys* 1999 Aug; **26**(8): 1589-99. PubMed PMID:10501059.
5. Hillen B, Hoogstraten HW, Post L. A mathematical model of the flow in the circle of Willis. *J Biomech* 1986; **19**(3): 187–194. PubMed PMID: 3700431.
6. Cassot F, Vergeur V, Bossuet P, et al. Effects of anterior communicating artery diameter on cerebral hemodynamics in internal carotid artery disease. A model study. *Circulation* 1995 Nov 15; **92**(10): 3122-31. PubMed PMID: 7586284.
7. Lankhaar JW, Westerhof N, Faes TJ, et al. Qantification of right ventricular afterload in patients with and without pulmonary hypertension. *Am J Physiol Heart Circ Physiol* 2006 Oct; **291**(4): H1731-7. Epub 2006 May 12. PubMed PMID: 16699074.
8. Kluytmans M, van der Grond J, van Everdingen KJ , *et al.* Cerebral hemodynamics in relation to patterns of collateral flow. *Stroke* 1999 Jul; **30**(7): 1432-9. PubMed PMID: 10390319.
9. Mut F, Aubry R, Löhner R, Cebral JR. Fast Numerical Solutions of Patient-Specific Blood Flows in 3D Arterial Systems. *Int J Numer Method Biomed Eng* 2010 Jan; **26**(1): 73-85. PubMed PMID: 21076685; PubMed Central PMCID:PMC2978074.
10. Wang JJ, Parker KH. Wave propagation in a model of the arterial circulation. *J Biomech* 2004 Apr; **37**(4): 457–70. PubMed PMID: 14996557.
11. Ursino M, Giannessi M. A model of cerebrovascular reactivity including the circle of willis and cortical anastomoses. *Ann Biomed Eng* 2010 Mar; **38**(3): 955-74. doi: 10.1007/s10439-010-9923-7. Epub 2010 Jan 22. PubMed PMID: 20094916.
12. Nardinochini P, Pontrelli G, Teresi L. A one-dimensional model for blood flow in pre stressed vessel. *Eur J Mech* 2005; **24**: 23–33.
13. Torii R, Oshima M, Kobayashi T. Computer modeling of cardiovascular fluid-structure interactions with the deforming spatial domain-time formulation. *Computer methods in Applied Mechanics and Engineering* 2005; **13**: 549–57.
14. Guyton AC. *Text book of physiology.* 9th ed. Philadelphia : W.B. Saunders 1996.
15. Olufsen MS, Nadim A. On deriving lumped models for blood flow and pressure in the systemic arteries. **Math Biosci Eng** 2004 Jun; **1**(1): 61-80. PubMed PMID: 20369960.
16. Hassani K, Navidbakhsh M, Rostami M. Simulation of the cardiovascular system using equivalent electronic system. *Biomed Pap Med Fac Univ Palacky Olomouc Czech Repub* 2006 Jul; **150**(1): 105-12. PubMed PMID: 16936911.
17. Alastruey J, Parker KH, Peiró J, Byrd SM, Sherwin SJ. Modelling the circle of Willis to assess the effects of anatomical variations and occlusions on cerebral flows. *J Biomech* 2007; **40**(8): 1794-805. Epub 2006 Oct 11. PubMed PMID: 17045276.
18. Rideout VC. *Mathematical and computer modeling of physiological systems.* Illustrated ed. New York : Prentice Hall 1991.
19. O'Rourke M. Accurate Measurement of Arterial Pressure. *J Hum Hypertension* 2003 Jul; **17**(7): 445-7. PubMed PMID: 12821949.
20. Cieslicki K, Ciesla D. Investigations of flow and pressure distributions in physical model of the circle of Willis. *J Biomech* 2005 Nov; **38**(11): 2302-10. Epub 2004 Dec 13. PubMed PMID: 16154418.